


 Cite this: *RSC Adv.*, 2021, **11**, 9840

Facile multifunctional IOL surface modification *via* poly(PEGMA-co-GMA) grafting for posterior capsular opacification inhibition†

Jiayi Xia, Duoduo Lu, Yuemei Han, Jiahao Wang, Yueze Hong, Peiyi Zhao, Qiuna Fang and Quankui Lin *

Posterior capsule opacification (PCO) is a significant complication of intraocular lens (IOL) implantation in cataract surgery, in which the adhesion and proliferation of lens epithelial cells (LECs) on the implanted IOL surface play an important role. The surface modification of IOL to prevent LEC adhesion and proliferation is a practical way to reduce the incidence of PCO. In this study, a multifunctional binary copolymer of poly(ethylene glycol) methacrylate (PEGMA) and glycidyl methacrylate (GMA) was synthesized (poly(PEGMA-co-GMA), PPG) and chemically grafted onto the aminolyzed IOL surface, utilizing the coupling reaction of epoxy and amino groups. Doxorubicin (DOX) was subsequently immobilized on the surface coating *via* the reaction of epoxy and amino groups as well. Taking advantages of the hydrophilicity of the PEG segments in the copolymer coating and the anti-proliferative effects of the DOX, a multifunctional surface coating was easily established by the synthesized copolymer PPG. Such anti-proliferative drug immobilized hydrophilic coating modification may effectively reduce the cell adhesion and proliferation and thus it is hypothesized to have great potential in PCO inhibition. The synthesis of PPG was confirmed by proton nuclear magnetic resonance spectroscopy (¹H-NMR) and Fourier transform infrared spectroscopy (FTIR). The surface coating immobilization was demonstrated by X-ray photoelectron spectroscopy (XPS). The *in vitro* drug release profiles and the cell behaviors were also investigated to validate the multifunctional coating inhibition effect on cellular adhesion and antiproliferation. Finally, the *in vivo* ocular implantation was carried out on rabbit eyes to evaluate the effect of the coating modified IOL on the inhibition of postoperative PCO. It followed that such multifunctional coating modification can effectively inhibit the adhesion and proliferation of LECs and significantly reduce the incidence of PCO. All these results reveal that such PPG copolymer modification provides a facile yet effective way to inhibit PCO formation after IOL implantation.

 Received 10th January 2021
 Accepted 2nd March 2021

 DOI: 10.1039/d1ra00201e
rsc.li/rsc-advances

1. Introduction

Cataracts are the leading cause of blindness in the world.¹ It is estimated that almost 95 million people are affected by cataracts, in particular in developing countries.² Currently, the most common treatment for cataracts is phacoemulsification, combined with the implantation of an intraocular lens (IOL).^{3,4} However, for the human body, the IOL is a foreign implant, and thus has the potential to cause postoperative complications. The most common postoperative complication after IOL implantation is posterior capsular opacity (PCO), which is also known as a second cataract. Five years after surgery, the incidence of PCO is approximately 28.4% in adults, while it is almost 100% in children.^{5–7} The main mechanism of PCO is the

adhesion, proliferation, migration, and epithelial-mesenchymal transformation of the residual lens epithelial cells (LECs) in the lens capsule after surgery. This cellular behaviour causes the formation of a translucent membrane on the posterior capsule or IOL, which leads to a decrease in the patient's vision after surgery.⁸ To date, the only effective treatment for PCO is neodymium-doped yttrium aluminum garnet (Nd:YAG) laser capsulotomy.^{9,10} However, this surgery not only increases the financial burden but also brings new complications, such as IOL damage, macular cystic edema, or retinal detachment. In addition, because of the need for precise focus, this surgery is not suitable for children.^{11,12} Therefore, the prevention of posterior cataracts is particularly important.

Surface modification of the biomaterials provides an effective way to improve their biocompatibilities. There were also plenty of investigations on the IOL surface modification to reduce the PCO applications, which mainly focused on surface hydrophilization by tethering hydrophilic molecules, which can reduce the LEC adhesion onto IOL.^{13–15} However, our previous

School of Ophthalmology & Optometry, Eye Hospital, Wenzhou Medical University, 270 Xueyuan Road, Wenzhou 325027, China. E-mail: lingk@wmu.edu.cn

† Electronic supplementary information (ESI) available. See DOI: [10.1039/d1ra00201e](https://doi.org/10.1039/d1ra00201e)



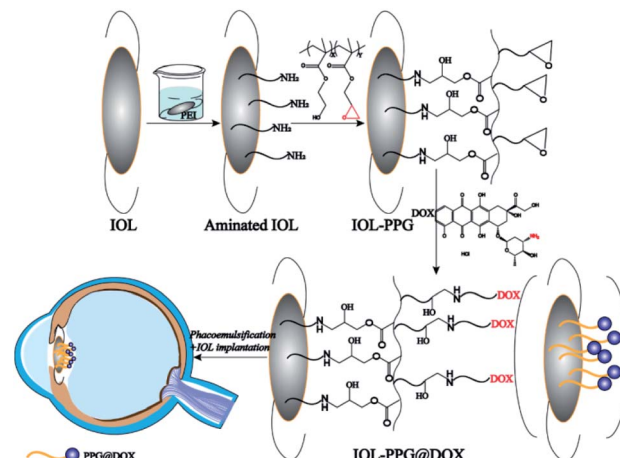
investigations found out that solely hydrophilic surface modification only delayed the PCO occurrence but can't eliminate the PCO incidence.¹³ Clinical trials have also shown that there is no significant difference in the long-term PCO incidence between the heparinized IOLs or the pristine IOLs.¹⁶ On the other hand, local drug administrations, mainly including adding drugs to the lavage fluid intraoperatively,¹⁷ anterior chamber anti-proliferative drug injection after operation and anti-inflammatory eye drops administration postoperatively,¹⁸ were also carried out aiming to decrease the proliferation of the residual LECs. However, owing to the low drug bioavailability and fast drug metabolism, these administrations often lead to excessive local drug concentration, serious side effects to the surrounding tissues. Moreover, the drug has a short time of action, which has no pronounced effect on the reduction of the PCO incidence.^{19–21} As a intraocular implant, IOL can be served as a drug delivery reservoir.²² The drug eluting IOL has been developed by several methods, including the IOL soaking in the antibiotics solution, as well as surface modification with a doxorubicin (DOX) incorporated nanoparticle loaded poly-electrolyte multilayer coating.^{23–26} The drug eluting IOL presents good *in situ* therapeutic effects of the loaded drugs.^{25,26} As a result, multifunctional surface coating modification of IOL with synergistic properties of anti-adhesion and anti-proliferation may have great potential in effectively inhibiting the PCO incidence after cataract surgery.

In present investigation, a facile yet effective surface modification method was developed to fabricate an anti-adhesion and anti-proliferation multifunctional coating on the IOL. Binary copolymer of poly(ethylene glycol) methacrylate (PEGMA) and glycidyl methacrylate (GMA) was synthesized (poly(PEGMA-*co*-GMA), PPG) for surface modification applications. Taking advantages of the reactive activities of the epoxy group in the GMA part, the PPG copolymer can be easily grafted with the amino group contained materials or molecules.²⁷ On the other hand, the PEGMA part in the PPG copolymer provides good hydrophilicity which could effectively prevent the attachment of non-specific proteins and inhibits cell attachment.^{28–31} As a result, the PPG copolymer was chemically grafted onto the aminolyzed IOL surface, utilizing the coupling reaction of epoxy and amino groups. The doxorubicin (DOX) was subsequently immobilized on the surface coating *via* the reaction of epoxy and amino groups as well. Taking advantages of the hydrophilicity of the PEG segments in the copolymer coating and the anti-proliferative effects of the DOX, a multifunctional surface coating was easily established by PPG modification (Scheme 1). Such anti-proliferative drug immobilized hydrophilic coating modification may effectively reduce the cell adhesion and proliferation and thus it is hypothesized to have great potential in the PCO inhibition.

2. Experimental section

2.1 Materials

The polyethylene glycol methacrylate (PEGMA, $M_n = 360$), glycidyl methacrylate (GMA), azodiisobutyronitrile (AIBN), inhibitor removers, doxorubicin hydrochloride (DOX), poly(ethylene

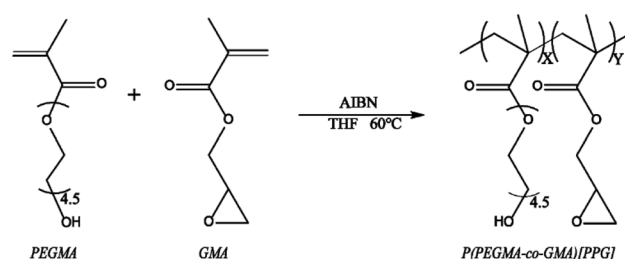


Scheme 1 Flow chart of hydrophilic drug-loading coating was constructed on the IOL surface.

imine) (PEI) and fluorescein diacetate (FDA) were purchased from Sigma-Aldrich. Ethanol, methanol and tetrahydrofuran (THF) were obtained from JinShan Reagent. Cell culture medium DMED/F12 (1 : 1), fetal bovine serum (FBS), penicillin-streptomycin, 0.05% trypsin-EDTA, phosphate buffer saline (PBS) and hanks solution were bought from Invitrogen. The hydrophobic acrylic foldable IOLs used in the animal experiments were provided by 66 Vision-Tech Co., Ltd. (66VT®, FV-60A, the diameter of the optical region was 6 mm). The human lens epithelial line (HLE B3, CRL-11421™) was originally obtained from American Type Culture Collection (ATCC) (Manassas, VA, USA). All the Japanese White rabbits used in the animal experiments were obtained from the animal centre of Wenzhou Medical University. All the eye drops used on animals after operation were obtained from the Eye Hospital of Wenzhou Medical University. The inhibitor remover was used to remove the hydroquinone and monomethyl ether hydroquinone in the PEGMA before use. All other chemical reagents were analytically pure and did not require further purification before usage.

2.2 Synthesis of poly(PEGMA-*co*-GMA) (PPG)

As showed by Scheme 2, the binary copolymer PPG was synthesized by conventional radical polymerization of PEGMA and GMA with AIBN as the initiator.²⁸ Briefly, 0.25 mM PEGMA, 0.25 mM GMA and 0.0083 mM AIBN were dissolved in 10 mL THF/methanol (v/v = 7/3) mixed solvent under vigorously



Scheme 2 The synthesis procedure of PPG.



stirring. Then the mixture solution was transferred in to a flask, sealed and drained with nitrogen for 20 min to remove oxygen. Then, polymerization reaction was carried out at 60 °C for 12 h. After the reaction, the reaction mixture was transferred into dialysis bag (MWCO = 3500) and dialyzed in ultrapure water for 72 h. The dialysis products were lyophilized for 48 h and the pure PPG was obtained. The obtained PPG was dissolved in deuterium chloroform at a concentration of 10 mg mL⁻¹. 0.6 mL of the solution was injected into a nuclear magnetic resonance (NMR) tube and the ¹H-NMR spectra were obtained by a 400M NMR spectrometer (Quantum-I plus, Wuhan Zhongke Oxford Spectrum Technology Co. Ltd). On the other hand, a drop of PEGMA or GMA monomer was dropped on the sample table and measured using the transmission mode of the FTIR. 10 mg PPG was placed in the laminating device which was placed on the infrared laminating machine, the pressure was adjusted to 1 ton, and after holding for 2 minutes, the obtained PPG sheet was measured with the transmission mode of FTIR (Nicolet iS20, Thermo Fisher Technologies Inc.).

2.3 Surface modification and characterization

The IOLs as well as medical polyester material polyethylene terephthalate, silicon wafer and quartz slice were used as surface modification substrates in the investigation for requirements of various coating characterizations. The surface medication process was carried out at room temperature. Briefly, the substrates were ultrasonic cleaned by ethanol and water successively. Each cleaning step is 5 min and repeated twice. Then the substrates were soaked in 3 mg mL⁻¹ PEI aqueous solution for 24 h to generate aminated substrate (defined as \sim NH₂). It was further incubated in 1 mg mL⁻¹ PPG solution (in methanol) for another 24 h, rinsed by methanol and water rinsing twice successively. Thus the PPG grafted substrate (defined as \sim PPG) was obtained *via* ring opening reaction of amine group to epoxy group. The PPG grafted substrates were then immersed in 0.5 mg mL⁻¹ DOX aqueous solution avoid light for 24 h, which facilitate the DOX grafting onto the residual epoxy groups on the PPG chain in the surface. The products were washed with water for three times, followed by nitrogen blowing for desiccation. Thus the DOX immobilized PPG grafted substrates were obtained (defined as \sim PPG@DOX).

The X-ray photoelectron spectroscopy (XPS, ESCALAB 250Xi, PerkinElmer Co., America), scanning electron microscopy (SEM, PW-100-160, Thermo Fisher Scientific, USA), static water contact angle (SWCA, OCA 15 EC, DataPhysics, Germany) were used to characterize the changes of chemical elements, morphology and wettability on the surface during the surface modification. The UV-vis spectrophotometer (UV-1780, SHIMADZU, Japan) was used to investigate the light transmittance of the surface modified IOLs.

2.4 In vitro drug release profiles investigation

To monitor the drug delivery behaviours of the fabricated multifunctional coating modified IOLs, the *in vitro* drug release profiles were carried out in PBS (pH = 7.4) or NaAc buffer solution (pH = 5.5), aiming to simulate the *in vivo* normal

physiological and pathological environment respectively. The multifunctional coating modified IOL materials were placed in vials with 3 mL release buffer and incubated in the 37 °C constant temperature shaking incubator. 1 mL of the released buffer was collected at certain time point and stored at 4 °C. Meanwhile, some volume of the fresh release buffer was added into the vials simultaneously. The release buffer was collected at 1 h, 2 h, 4 h, 5 h, 8 h, 12 h, 24 h, etc. The release process was last for as long as 168 h. After collection, 200 μ L of the release buffer was added into a photophobic 96-well plate and the fluorescent optical density (OD) was read under excitation wavelength of 490 nm and emission wavelength of 590 nm by microplate reader (SpectraMax M5, Bio-Rad, USA).

2.5 *In vitro* cell behaviours investigation

The LECs were cultured in DMED/F12 medium supplemented with 10% FBS and 1% penicillin-streptomycin at 37 °C in a humidified atmosphere with 5% CO₂. The LECs were recovered, cultured, and passaged according to a standardized manner. Pristine, aminated (\sim NH₂), PPG grafted (\sim PPG), and DOX immobilized PPG grafted (\sim PPG@DOX) IOL materials were loaded in 96-well plate and sterilized under ultraviolet light for 2 h before use. 5 \times 10³ cells in 200 μ L complete medium were seeded into the wells and incubated for 48 and 72 h. At each time interval, 20 μ L FDA solution (2 μ g mL⁻¹) was added into the wells and incubated for 15 min, followed by gentle PBS washing three times. The morphology of the cells on the substrates was observed by fluorescent microscopy (Axiovert a3, German Zeiss) through the filter that are excited at 488 nm and emitted at 525 nm. The cell number was calculated by ImageJ as well.

2.6 Animal experiments

All animal procedures were performed in accordance with the Guidelines for Care and Use of Laboratory Animals of "Wenzhou Medical University" and approved by the Animal Ethics Committee of "Wenzhou Medical University". Twelve Japanese White rabbits with two-month-old were used and they were equally divided into two groups. Phacoemulsification combined with IOL implantation surgery was performed on a phacoemulsification instrument (Laureate, World phaco system, Alcon Laboratories, Inc) by Dr Han Yuemei. All the surgical materials as well as instruments were sterilized with ethylene oxide. The phacoemulsification and IOL implantation procedure was the same with our previous publications.³² Briefly, the multifunctional coating modified IOLs were implanted into the right eyes of the rabbits after the cortex removing by the phacoemulsification, with polishing step omitted for easier establishing the PCO model. The pristine IOLs were also implanted as controls in another group of rabbits. In the first and second week after the operation, the surgical eyes were administrated with eye drops, including levofloxacin, tropicamide, and compound tobramycin-dexamethasone. The intraocular pressure (IOP) of the surgical eyes was measured at different time points after operation. The slit lamp was taken to observe the acute post-operative inflammatory reaction and the long term PCO



developing situation on the IOL surface. Electroretinogram (ERG, RETI-Port21, Roland, Germany) was taken by Retinal electrophysiological instrument for assessing biosafety of the multifunctional coatings on the IOLs. After placed in a dark environment for four hours, ERG of the dark adaption at modes of 0.01, 3.0, 10.0 Hz and light adaption at modes of 3.0 Hz and Flicker were tested. The rabbits were anesthetized and sacrificed at postoperatively eight weeks. The eyes were extracted and fixed in 4% paraformaldehyde. The Miyake Apple view images of lens capsule with IOLs were taken by Stereomicroscope which directly showed the process of intra-capsular hyperplasia. Then, the cornea, iris, lens capsule, and retina were separated under a surgical microscopy, soaked in a sucrose solution for dehydration for 24 h, followed by frozen section and hematoxylin-eosin staining.

2.7 Statistical analysis

Three parallel samples were used for each experiment. The results obtained were averaged, and the standard deviation was calculated. A *t*-test was used to compare the statistical significance. *P* < 0.05 was considered that there is a significant difference.

3. Results and discussion

3.1 PPG synthesis and surface modification

As showed by Scheme 1, the binary copolymer PPG was synthesized by conventional radical polymerization of PEGMA and GMA. The FTIR and ¹H-NMR were used to demonstrate the successful synthesis of the PPG copolymer. As shown in Fig. 1, characteristic peaks at 950 and 842 cm⁻¹ were found in GMA monomer, which were attributed to the unsymmetrical expansion and contraction vibrations of the epoxy groups (Fig. 1A). Also, characteristic peaks at 1725 and 1112 cm⁻¹ at PEGMA monomer were correspond to the tensile vibrations of the ester groups C=O and C-O-C respectively (Fig. 1B).^{21,28} These characteristic peaks were also shown in the resulted products (Fig. 1C), which illustrated that the copolymer contains GMA

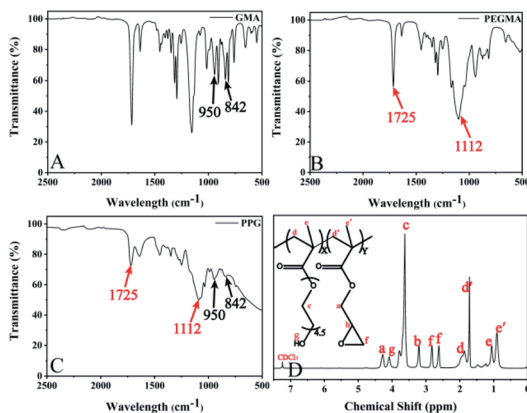


Fig. 1 (A), (B) and (C) are FTIR spectra of GMA, PEGMA and copolymer PPG respectively. (D) ¹H-NMR spectrum of PPG dissolved in chloroform-d solution.

and PEGMA fragments. This was also confirmed by ¹H-NMR analysis (Fig. 1D), in which the chemical shift at $\delta = 4.3$ corresponds to the methyl group adjacent to the epoxy group on GMA, and the chemical shift at $\delta = 3.6$ is due to the CH₂-CH₂-O group of PEGMA.^{33,34} All results indicated the successful synthesis of PPG.

The synthesized PPG copolymer was then used to surface modify the IOL materials and which also facilitated the subsequent DOX immobilization. The surface modifications within each step were demonstrated by XPS. As shown in Fig. 2A, there was virtually no characteristic peak of N element on pristine substrate surface. While after the PEI treating, the peak at 401 eV attributed to N_{1s} appeared on the surface, indicating that the amination process was successfully carried out. When PPG was grafted onto the surface, the intensity of N signal decreased because PPG did not contain nitrogen whereas as the XPS detection limitation is on the level of nano-scale. After the reaction with DOX solution, the content of N was further reduced because the N composition in DOX was lower than that in PPG modified substrate. Fig. 2B, C, and D shows the fine spectral peaks of the C elements of pristine, ~PPG and ~PPG@DOX respectively, where the peaks with binding energies (BEs) at 284.6, 286.2, and 288.7 eV correspond to the C in the hydrogen carbon (C-H and C-C), ether (C-O), and carbonyl (O-C=O) respectively.^{34,35} Compared with pristine substrate, a new peak with the BEs at 288.7 eV appeared and the peak at 286.2 eV increased dramatically in the PPG modified substrate, which indicates the successful introduction of the PPG onto the surface, as the PPG contain a lot of ester bonds from the PEGMA and GMA segment, as well as a large number of C-O bonds in the PEGMA segment. In the PPG@DOX modified substrate, the peak at 284.6 eV increased because the content of the hydrogen carbon (C-H and C-C) in DOX was higher than that in PPG modified surface. These results indicate that the drug immobilized multifunctional polymer coating was successfully grafted on the material surface.

The surface wettability during the coating modification was also determined. It can be seen that the surface hydrophilicity was improved gradually when the modification process

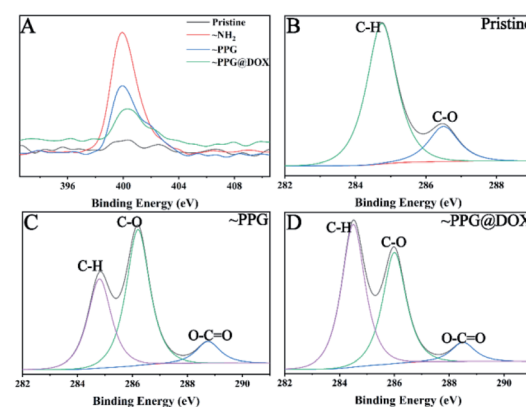


Fig. 2 The fine XPS spectra of material surface modifications. (A) N_{1s} spectra; (B), (C) and (D) are the C_{1s} spectra of pristine, ~PPG and ~PPG@DOX surfaces respectively.



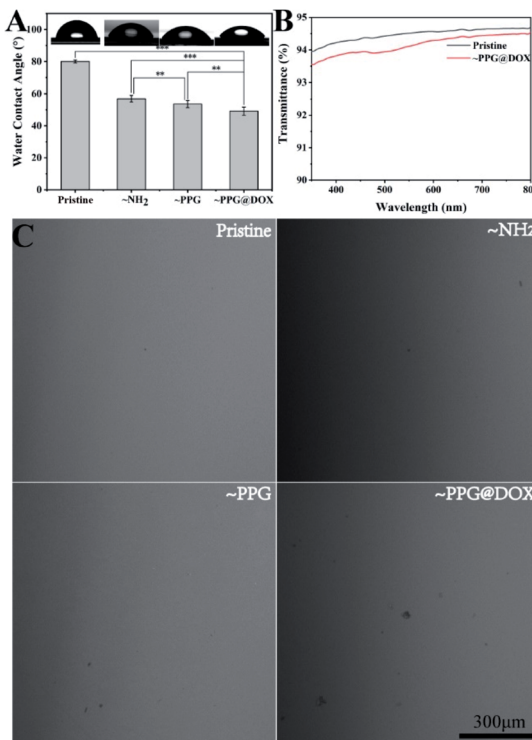


Fig. 3 Water contact angel (A), light transmittance (B) and representative surface morphology (C) of IOL materials in the process of modification. ** indicates $p < 0.01$, *** indicates $p < 0.001$.

continues (Fig. 3A). The pristine substrate was a relatively hydrophobic material, with WCA above 80° . It decreased to $56.8 \pm 1.9^\circ$ after amination was generated on the surface. The WCA continued to decrease after PPG copolymer or subsequently DOX grafting, with WCA value lower than 50° was detected on these surfaces. The increased surface hydrophilicity after PPG or DOX@PPG grafting was mainly due to the PEG segment in the copolymer, which may have positive effects in the inhibition of the cell adhesions.³⁶

As the lens is one of the most important refractive tissues in the eyeball, therefore, the surface properties is an important issue should be considered when surface modification. The material surface morphology in each step was investigated by SEM (Fig. 3C). As shown in Fig. 3C, in each step of the modification process of the drug-carrying polymer coating, the surface morphology of the material did not change markedly, indicating that the multifunctional drug immobilized coating modification had no significant influence on the surface morphology of the material. The light transmittance evaluation result also revealed that such multifunctional coating modification did not influent the light transmission, of which the light transmittances were both over 90%.

3.2 *In vitro* drug release

The drug release behaviours were then investigated. As shown in Fig. 4, the drug release profiles of IOLs with drug loaded multifunctional coating modification present a biphasic

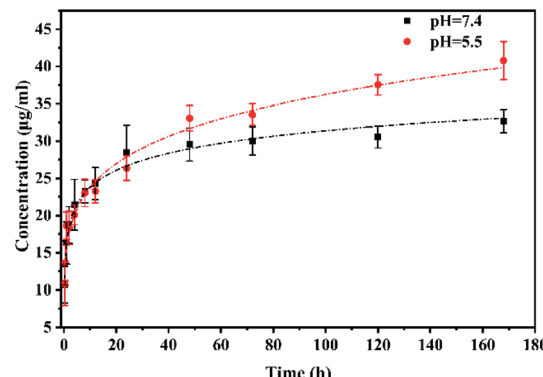


Fig. 4 Drug release process in buffer solution with $\text{pH} = 7.4$ and $\text{pH} = 5.5$ of coating modified IOL.

sustained release process. There were burst releases found in both normal physiological ($\text{pH} 7.4$) and pathological ($\text{pH} 5.5$) conditions in the first 12 h. The burst release of the drug in the early stage may meet the effective therapeutic concentration of the drug in the microenvironment when actual application. Besides, pH dependent release profiles were found when the incubation time increasing. The drug on the multifunctional coating was trend to release faster in the pathological condition than that in the physiological condition. The UV-Vis spectra of the DOX@PPG modified materials (Fig. S1†) and the $^1\text{H-NMR}$ spectra of the materials before and after released for one week (Fig. S2†) confirmed the pH sensitive release profile of the DOX from the DOX@PPG modified surface. The characteristic peaks of the DOX decreased much more evident in the $\text{pH} 5.5$ comparing with that in the $\text{pH} 7.4$ after 7 days releasing. On the other hand, there are still significant DOX remained on the material surfaces, as there are obvious rest peaks found on the spectra. The sustained release was found as long as 30 days in this situation. There was still characteristic DOX signal found on the materials (Fig. S3†), which means the drug was sustained release from the materials and the release time was longer than one month. This pH-sensitive release behaviour of the DOX conjugated poly(glycidyl methacrylate) has also found in other investigation previously.³⁷⁻⁴⁰ It is reported that the microenvironment in cell proliferative condition mainly presents slight acidic.⁴¹ Thus the pH dependent drug eluting property in this multifunctional coating may have great potential in the PCO prevention after IOL implantation.

3.3 *In vitro* cell behaviour

Postoperative adhesion and proliferation on the lens of residual LECs play a key role in the occurrence of PCO. Therefore, the anti-adhesion and anti-proliferation effects of the multifunctional coating modified surfaces on LECs *in vitro*. It can be seen from the cell density calculation (Fig. 5A) that there were no significant differences among the TCPS, unmodified pristine and aminated surfaces, no matter detected in the 48 h or 72 h after cell seeding. The cell density was decreased when the multifunctional coating was generated on the surface. The significantly decreased cell density was obtained on the PPG modified surface after 48 h. The mechanism of the effective



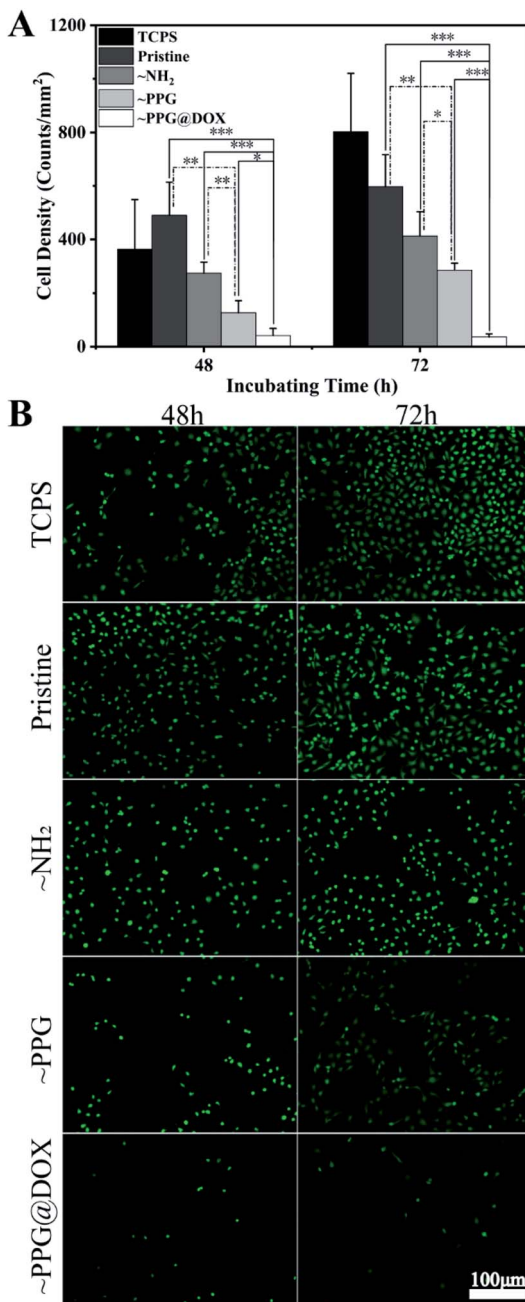


Fig. 5 (A) Adhesion density of cells on the surface (* $P < 0.05$, ** $P < 0.01$, *** $P < 0.001$); (B) fluorescence microscopy of HLEB3 on different surface with TCPS, pristine substrate, $\sim\text{NH}_2$, $\sim\text{PPG}$ and $\sim\text{PPG@DOX}$ after FDA staining.

prevention of cell attachment of this surface coating is due to the PEG moieties in the copolymer chains, which was proved to have distinct non-specific cell and protein resistant property.¹³ However, the small amount adherent cell on the PPG surface also proliferated well on such surface, with increased adherent cell density was found from 48 h to 72 h. On the contrary, the subsequent DOX immobilization on the surface greatly inhibits the cell proliferation. The cell density on the surface was extremely low in such surface, not only found after 48 h but also after 72 h' incubation. The Fig. 5B shows the representative

fluorescent images of the live cells on the different surfaces, which were well agreed with the above quantitative results. It can also be seen that the adherent cells spreading well on each PPG coated surface, indicating that the good biocompatibility of the coating material. These results demonstrate that the drug loaded multifunctional coating is not only biocompatible but also able to inhibit the LECs adhesion and proliferation on the surface.

3.4 Anti-PCO evaluation and *in vivo* biocompatibility

The *in vivo* biological environment is far more complex and changeable than the external environment. In order to understand whether the multifunctional coating modified IOL can prevent PCO *in vivo*, the intraocular implantation was carried out. Through slit lamp observation, as shown in Fig. 6, it can be seen that the inflammatory reaction was mild in the first week after the operation and disappeared after one week in both pristine and coating modified IOL groups. In the second week after the operation, cell proliferation was already observed around the posterior capsule and IOL surface in the pristine IOL group, as indicated by the red and black arrows in figures, telling that PCO had started to develop. On the contrary, no cell proliferation was observed in the surface modified IOL cases. In the fourth week after surgery, the LECs of the pristine IOL group

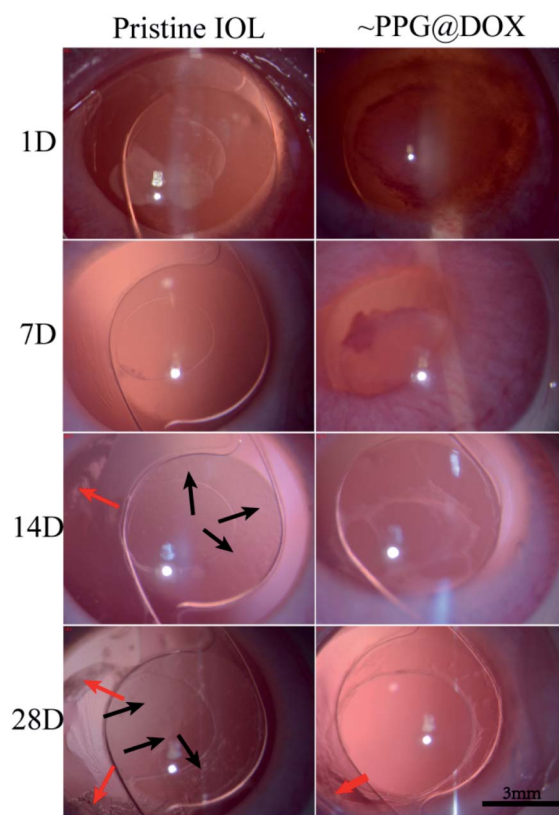


Fig. 6 Representative slit lamp microscopic images of pristine IOL and $\sim\text{PPG@DOX}$ modified IOL implanted rabbit eyes at 1D, 7D, 14D and 28D after surgery. The red arrows represent soemmering rings at equatorial part of capsule. The black arrows indicate the cells proliferation on IOL surface.

gradually migrated and proliferated in the central optical region between IOL and posterior capsule, whereas the optical region of the surface modified IOL group still remained transparent and no cell proliferation was observed. These results indicate that such drug loaded multifunctional coating modified IOL can prevent PCO formation effectively. On the other hand, there were some soemmering rings (SR) found at equatorial part of capsule in the surface modified IOL group, which can told from one side that such surface drug eluting coating only effective to induce cell apoptosis on the IOL surface whereas keeps good safety to the surrounding tissues, even the equatorial region away from the IOL in the lens capsule.

In order to show the PCO severity more intuitively, the IOLs within the lens capsule were isolated from the eyeballs and the stereomicroscopic and histological section images were taken. In order to evaluate the severity of PCO accurately, PCO was classified into SR, periphery posterior capsule opacification (PPCO) and central posterior capsule opacification (CPCO). Since the postoperatively residual LECs are initially located at the equator, the cells start multiplying at the equator and they produce a lot of extracellular matrix, forming SR. PPCO was formed when LECs migrate to the surrounding optical part of IOL which represents the area 3–6 mm away from the centre of

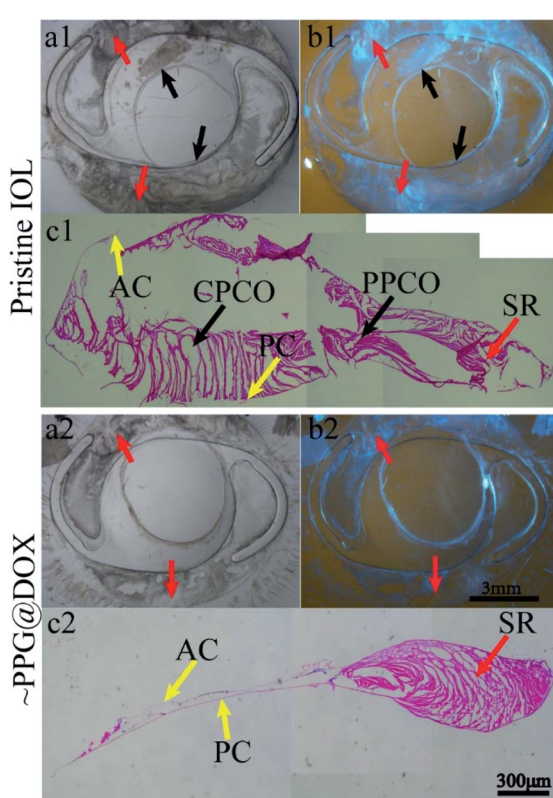


Fig. 7 (a1, a2) and (b1, b2) are stereomicroscopic images of capsules with pristine and multifunctional IOLs implanted respectively. (c1) and (c2) are histological section images of the capsule of the above two groups. Red arrows represent SR at equatorial part of capsule. Black arrows indicate the cells proliferation on IOL surface. PC: posterior capsule; AC: anterior capsule; PPCO: periphery posterior capsule opacification; CPCO: central posterior capsule opacification; SR: soemmering rings.

Table 1 IOP of rabbits' eyes at different operative time

Groups	3D	7D	14D	21D	28D
Pristine IOL	8.56 ± 4.30	8.56 ± 2.59	8.00 ± 2.65	7.22 ± 1.17	8.00 ± 1.41
IOL-	10.00 ±	6.89 ±	7.44 ±	5.78 ±	8.22 ±
PPG@DOX	1.45	1.02	1.64	0.19	1.16
P	0.611	0.358	0.773	0.103	0.909

IOL. When LECs migrate to an area within central optical part of the IOL (diameter = 3 mm), it leads to CPCO. From the Fig. 7, it can be seen that there were soemmering rings formed in both groups, which was consistent with the above slit lamp results (Fig. 7(a1, a2) and (b1, b2)). In pristine IOL group, extensive cell proliferation and fibrosis were observed at peripheral (PPCO) and central (CPCO) parts of the IOL (Fig. 7(c1)), while there was almost no PPCO and CPCO were found in PPG@DOX modified IOL group (Fig. 7(c2)). These results verified again that multifunctional coating modified IOL could effectively inhibit PCO formation after implantation.

As a drug eluting implantable materials, *in vivo* biocompatibility and the biosafety always been an important theme apart from the effectiveness. Herein, the *in vivo* biocompatibility and biosafety were also further verified by the histomorphological observation of the intraocular surrounding tissues and the visual function, as well as the IOP measurement after implantation. It can be seen from the postoperatively IOP measurement that there was no significant difference between the eyes with pristine or multifunctional surface coating modified IOLs (Table 1), telling that such surface modification would not cause elevated IOP after surgery. Then, histological sections of cornea, iris, and retina observation results also showed that the surface modified IOLs does not cause histomorphological changes to the intraocular neighbouring tissues (Fig. 8), indicating the good biocompatibility of the surface coating modifications. Retinal electrophysiologic function is an objective method to determine visual function. Herein, ERG was carried out to test the biosafety of the surface modification coatings after implantation. It can be seen from Fig. 9 that there was no statistical difference ($p > 0.05$) of the sum amplitude of

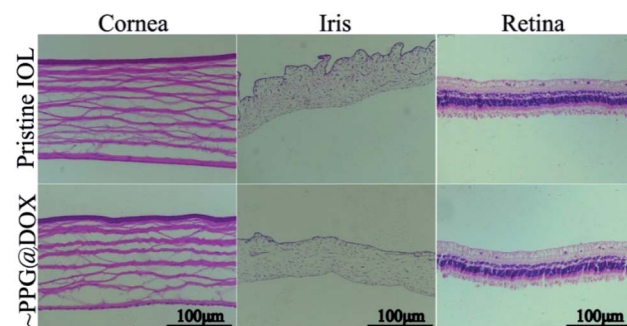


Fig. 8 Representative histological section images of cornea, iris and retina from the eyes with pristine and surface modified IOL implantation.



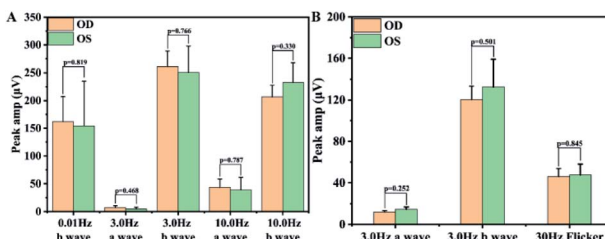


Fig. 9 Comparison of peaks in each stage of ERG between the surface modified IOL implanted eyes (OD) and normal eyes (OS). (A) Dark adaption; (B) light adaption.

oscillatory potential and the amplitudes of 'a' wave and 'b' wave between eyes with the pristine and surface modified IOLs implantation, which revealed that such surface modification has no side effects on retinal function. All these results indicated that the prepared multifunctional IOL has good biocompatibility and can be safely applied *in vivo*.

As PCO is a complication with high incidence after IOL implantation, the investigation and the surgical treatment to prevent PCO are always attracts the researchers' and the clinicians' attention. The surface hydrophilic modification of the IOL, such as heparinization, has clinically used for a long time aiming to reduce the PCO incidence.^{13,14} However, the clinically long term investigation has demonstrated that solely hydrophilic modification shows no significant differences when compared with the pristine IOLs. In present investigation, anti-proliferation design has introduced into the surface modification besides the hydrophilic surface coating. The multifunction of hydrophilicity and the anti-proliferation drug loading can be easily realized by the PPG copolymer immobilization. Such multifunctional surface coating renders efficient *in vivo* PCO inhibition. Although there is a long way from bench to bedside, such multifunctional surface coating with facile preparation characteristic may have great potential in the clinical applications.

4. Conclusions

The copolymer PPG with active epoxy group was successfully synthesized by conventional free radical polymerization and used to the surface modification of the IOL *via* the chemical conjugating between the epoxy groups and amino groups at room temperature. The anti-proliferative drug DOX can also be subsequently grafted onto the PPG coating *via* the residual epoxy group. Improved hydrophilicity and sustained drug release profiles with pH dependent release manner was found in such multifunctional coatings. Such multifunctional coating modification can well inhibit LECs adhesion and proliferation on the surface. The *in vivo* result indicated that such multifunctional coating modification has good biocompatibility and biosafety, yet it can inhibit the PCO development effectively after intraocular implantation. Compared with previous solely hydrophilic surface modification, such facile multifunctional IOL surface modification *via* poly(PEGMA-*co*-GMA) grafting provides a potential way to effectively inhibit the PCO development after IOL implantation.

Author contributions

Conceptualization, Q. K. L. and J. Y. X.; methodology, J. Y. X. and Q. K. L.; investigation, J. Y. X., D. D. L., Y. M. H., J. H. W., Y. Z. H., P. Y. Z., and Q. N. F.; writing—original draft preparation, J. Y. X.; writing—review and editing, Q. K. L.; supervision, Q. K. L.; funding acquisition, Q. K. L.

Conflicts of interest

There are no conflicts to declare.

Acknowledgements

The supports from the National Key R&D Program (2017YFC1104602), National Natural Science Foundation of China (81771984) were greatly acknowledged.

Notes and references

- D. Pascolini, S. P. Mariotti, G. P. Pokharel, R. Pararajasegaram, D. Etya'ale, A. D. Negrel and S. Resnikoff, *Ophthalmic Epidemiol.*, 2004, **11**, 67–115.
- Y.-C. Liu, M. Wilkins, T. Kim, B. Malyugin and J. S. Mehta, *Lancet*, 2017, **390**, 600–612.
- P. Jaycock, R. L. Johnston, H. Taylor, M. Adams, D. M. Tole, P. Galloway, C. Canning and J. M. Sparrow, *Eye*, 2007, **23**, 38–49.
- L. Lin, Q. Lin, J. Li, Y. Han, P. Chang, F. Lu and Y.-e. Zhao, *Biomater. Sci.*, 2019, **7**, 4208–4217.
- B. W. Findl O, P. Bauer and T. Sycha, *Cochrane Database Syst. Rev.*, 2010, **2**, CD003738.
- P. d. A. Jorge, D. Jorge, C. V. Ventura, B. V. Ventura, W. Lira, M. C. Ventura, M. R. Santiago and N. Kara-Junior, *Arq. Bras. Oftalmol.*, 2014, **77**, 222–224.
- D. A. Schaumberg, M. R. Dana, W. G. Christen and R. J. Glynn, *Ophthalmology*, 1998, **105**, 1213–1221.
- J. M. Marcantonio and G. F. J. M. Vrensen, *Eye*, 1999, **13**, 484–488.
- Y. Han, X. Xu, Y. Wang, S. Liu, X. Zhao, H. Chen and Q. Lin, *Colloids Interface Sci.*, 2018, **24**, 40–44.
- L. Cai, X. Han, Y. Jiang, X. Qiu, D. Qian, Y. Lu and J. Yang, *Am. J. Ophthalmol.*, 2021, **224**, 74–83.
- D. J. Apple, Q. Peng, N. Visessook, L. Werner, S. K. Pandey, M. Escobar-Gomez, J. Ram and G. U. Auffarth, *Ophthalmology*, 2001, **108**(3), 505–518.
- T. P. Werblin and D. Krider, *J. Cataract Refractive Surg.*, 2006, **32**, 373–374.
- Q. Huang, G. P. Cheng, K. Chiu and G. Q. Wang, *Chin. Med. J.*, 2016, **129**, 206–214.
- Q. K. Lin, J. M. Tang, Y. M. Han, X. Xu, X. J. Hao and H. Chen, *Colloids Surf., B*, 2017, **151**, 271–279.
- X. Huang, C. Luo, L. Lin, L. Zhang, H. Li, K. Yao and Z. Xu, *Mater. Sci. Eng., C*, 2017, **75**, 1289–1298.
- E. M. Krall, E. M. Arlt, G. Jell, C. Strohmaier, S. Moussa and A. K. Dexl, *J. Cataract Refractive Surg.*, 2015, **31**, 466–472.



17 A. L. G. Christine and M. Haus, *Br. J. Ophthalmol.*, 1996, **80**, 1087–1091.

18 L. Xie, J. Sun and Z. Yao, *Graefe's Arch. Clin. Exp. Ophthalmol.*, 2003, **241**, 309–313.

19 K. H. Eibl-Lindner, R. Liegl, C. Wertheimer and A. Kampik, *Ophthalmologe*, 2013, **110**, 990–994.

20 I. Lipnitzki, R. Bronshtein, S. Ben Eliahu, A. L. Marcovich and G. Kleinmann, *J. Ocul. Pharmacol. Ther.*, 2013, **29**, 414–418.

21 S. Garty, R. Shirakawa, A. Warsen, E. M. Anderson, M. L. Noble, J. D. Bryers, B. D. Ratner and T. T. Shen, *Invest. Ophthalmol. Visual Sci.*, 2011, **52**, 6109–6116.

22 S. Garty, R. Shirakawa, A. Warsen, E. M. Anderson, M. L. Noble, J. D. Bryers, B. D. Ratner and T. T. Shen, *Invest. Ophthalmol. Visual Sci.*, 2011, **52**, 6109–6116.

23 H. Huang, S. Zhu, D. Liu, S. Wen and Q. Lin, *J. Biomater. Sci., Polym. Ed.*, 2021, DOI: 10.1080/09205063.2020.1865691.

24 Y. Han, X. Xu, Y. Wang, S. Liu, X. Zhao, H. Chen and Q. Lin, *Colloid Interface Sci. Commun.*, 2018, **24**, 40–44.

25 L. Lin, Q. Lin, J. Li, Y. Han, P. Chang, F. Lu and Y.-e. Zhao, *Biomater. Sci.*, 2019, **7**, 4208–4217.

26 A. Topete, J. Tang, X. Ding, H. P. Filipe, J. A. Saraiva, A. P. Serro, Q. Lin and B. Saramago, *J. Controlled Release*, 2020, **326**, 245–255.

27 D. Luo, Y. Li and M. Yang, *J. Appl. Polym. Sci.*, 2011, **120**, 2979–2984.

28 Y. Wei, J. Zhang, H. Li, L. Zhang and H. Bi, *J. Biomater. Sci., Polym. Ed.*, 2015, **26**, 1357–1371.

29 L. Yu, Z. Z. Shi and C. M. Li, *J. Colloid Interface Sci.*, 2015, **453**, 151–158.

30 Y. Liu, C. X. Guo, W. Hu, Z. Lu and C. M. Li, *J. Colloid Interface Sci.*, 2011, **360**, 593–599.

31 Y. Liu, W. Wang, W. Hu, Z. Lu, X. Zhou and C. M. Li, *Biomed. Microdevices*, 2011, **13**, 769–777.

32 Y. M. Han, X. Xu, J. M. Tang, C. H. Shen, Q. K. Lin and H. Chen, *Int. J. Nanomed.*, 2017, **12**, 127–135.

33 S. Jiang, Y. Z. Poh and X. J. Loh, *RSC Adv.*, 2015, **5**, 71322–71328.

34 A. Venault, C.-S. Liou, L.-C. Yeh, J.-F. Jhong, J. Huang and Y. Chang, *ACS Biomater. Sci. Eng.*, 2017, **3**, 3338–3350.

35 D. Liu, J. Zheng, X. Wang, X. Lu, J. Zhu and C. He, *New J. Chem.*, 2018, **42**, 2248–2259.

36 X. Xu, J. M. Tang, Y. M. Han, W. Wang, H. Chen and Q. K. Lin, *J. Biomater. Appl.*, 2016, **31**, 68–76.

37 Q. L. Li, S. H. Xu, H. Zhou, X. Wang, B. A. Dong, H. Gao, J. Tang and Y. W. Yang, *ACS Appl. Mater. Interfaces*, 2015, **7**, 28656–28664.

38 R. Li, F. Feng, Y. Wang, X. Yang, X. Yang and V. C. Yang, *J. Colloid Interface Sci.*, 2014, **429**, 34–44.

39 L. Sun, Y. Zhou, X. F. Zhou, L. W. Ma, B. Y. Wang, C. Y. Yu and H. Wei, *ACS Appl. Polym. Mater.*, 2020, **2**, 2126–2133.

40 A. Pourjavadi, M. Kohestanian and M. Yaghoubi, *New J. Chem.*, 2019, **43**, 18656–18647.

41 I. Bertoncello, *Methods Protoc.*, 2019, **1940**, 23–30.

